FEEDBACK STABILIZATION OF MAGNETIC ISLANDS BY RF HEATING AND CURRENT DRIVE*

D. W. Ignat, P. H. Rutherford, and H. Hsuan

Princeton University

Plasma Physics Laboratory

P.O. Box 451

Princeton, NJ 08544, USA

PPPL--2278

DE86 002528

ABSTRACT

Feedback stabilization of the m = 2 mode in tokamaks would be advantageous for disruption-free operation at low q-values. Stabilization of the m = 1 mode and resulting "sawteeth" could lead to substantial increases in the stable β-value, as well as indirect stabilization of the m = 2 mode, by permitting q(0)-values below unity. Stabilization of these modes at acceptable amplitudes appears possible by feedback-modulated heating or current drive applied to the region within the mode-induced magnetic islands. Current drive offers by far the more efficient mechanism, and it can be accomplished using lower-hybrid or electron-cyclotron radio-frequency (rf) techniques. For the lower-hybrid case, ray-tracing calculations demonstrate the needed localization of the rf power, despite long ray paths in the toroidal direction. Top-launched lower-hybrid waves are favored for localized absorption.

*Invited paper presented at the "Course and Workshop on Applications of RF Waves to Tokamak Devices" (Varenna, Italy), September 5-14, 1985.

I. INTRODUCTION

The suppression of the m = 2 resistive-kink (tearing) mode in a tokamak would have three important advantages: (i) it could provide disruption-free operation at relatively low q(a)-values; (ii) it would provide a modest improvement in the limiting beta-value for ballooning instabilities by shortening the connection length [i.e., lowering q(a)]; and (iii) it would provide a modest improvement in confinement by allowing increased plasma current.

The successful suppression of the m = 1 mode and the associated "sawteeth" would have more substantial advantages: (i) it could provide a significant improvement in the limiting beta-value by reducing both $q(0)$ and q(a); (ii) it would provide indirect stabilization of the m = 2 mode (and other "external" resistive kinks) by allowing $q(0)$ to fall significantly below unity [corresponding to centrally-peaked $j(r)$-profiles that are known to be stable to $m \geq 2$ modes]; (iii) it would provide a significant improvement in confinement by allowing increased plasma current; and (iv) it would enhance the maximum ohmic heating power by increasing the central current density.

"Conventional" and "sawtooth-suppressed" tokamak profiles are illustrated schematically in Fig. 1. The conventional tokamak is restricted to q(a)-values not much below 3.0 because of conflicting requirements on the current profile: namely, that it provide stability against the $m = 2$ mode (and perhaps, also, the $m = 3$, $n = 2$ mode) and that $q(0)$ not be significantly below unity /1/. The sawtooth-suppressed tokamak might have q(a)-values of 2.0 or lower and $q(0)$-values as low as 0.7; the onset of higher-order "fractional-m/n" modes (e.g., $m = 3$, $n = 4$) would apparently preclude even lower $q(0)$-values /2/. The sawtooth-suppressed tokamak might be expected to exhibit a relatively flat pressure profile within the region $q(r) < 1$ because of the action of unstable resistive interchanges.

Feedback stabilization of $m \geq 2$ modes by rf heating and/or current drive has recently been proposed /3/, and extension of this technique to the m = 1 mode appears possible. To produce a stabilizing effect, the feedback technique must increase the plasma current density within the magnetic islands. There are two principal options for rf-feedback:

1. Heat the magnetic islands by localized rf heating, thereby lowering the resistivity;
2. Drive additional non-inductive currents within the magnetic islands.

In both cases, the rf power must be modulated in phase with the signal from a suitable detector. Feedback techniques based on electron-cyclotron heating (ECH) and lower-hybrid current drive (LHCD) are illustrated schematically in Fig. 2 for the case m = 1.

Island rotation can be detected by electron-cyclotron emission (ECE) and soft X-ray arrays for the m = 1 mode or by Mirnov coils for the m = 2 mode. The rotation of the modes is usually found to be in the electron diamagnetic drift direction, and in the Princeton Large Torus (PLT) it has a frequency around 2 kHz for the m = 2 mode and around 5 kHz for the m =1 mode. The rotation frequency becomes smaller for larger tokamaks. For the PLT, the heating pulse should be on the order of 50-100 μsec. This is easily achievable with a klystron amplifier for LHCD, and it is also attainable for ECH by using gun-anode modulators for a gyrotron oscillator.

The theory of feedback stabilization of tearing modes is summarized in Sec. II; a fuller account is given elsewhere /1/. Feedback by the (preferred) lower-hybrid current-drive technique is discussed in detail in Sec. III. The electron-cyclotron-heating technique is discussed in Sec. IV.

II. THEORY OF FEEDBACK STABILIZATION OF TEARING MODES

The theory of feedback stabilization of tearing modes by island heating follows the standard treatment of $m \geq 2$ modes in their slow-growing (nonlinear) phase, except that the resistivity on flux-surfaces interior to the island is allowed to be perturbed relative to that on exterior flux surfaces. The rf power density is modulated in phase with the rotating island,

$$P_{rf} = \tilde{P}_{rf} \cos(m\theta - n\phi - \omega t),$$

and the radial profile of power deposition is assumed to be quite narrow, but not as narrow as the island itself. The cross-field electron thermal diffusivity χ_e within the island limits the temperature perturbations that can be produced by the rf power.

The island width w is found to grow according to /1/

$$\frac{dw}{dt} = \eta\left(\Delta' - C_h \frac{\tilde{P}_{rf}}{\chi_e n T_e} w\right),$$

where Δ' is the usual measure of tearing-mode instability. The constant $C_h = 0.75(rj_z/B_\theta)(q/rq') \sim 0.5$, typically. If the feedback system can supply a

fraction f of the total heating power, depositing it within a region of radial width d, and if the local cross-field thermal diffusivity is comparable to its global value, $\chi_e = a^2/4\tau_{Ee} = a^2 P_{tot}/6nT_e$, then suppression of the islands requires

$$\Delta' a < 3\, f\, w/d,$$

implying that very large feedback power ($f \sim 1$) would be required to stabilize islands of width d in typical cases ($\Delta' a \sim 3$).

Feedback stabilization by island current drive requires a non-inductively driven current density modulated in phase with the rotating island:

$$j_{rf} = \tilde{j}_{rf} \cos(m\theta - n\phi - \omega t) .$$

The island width w is found to grow according to

$$\frac{dw}{dt} = \eta\left(\Delta' - C_d \frac{\tilde{j}_{rf}}{j_{zo}} \frac{1}{w}\right),$$

where $C_d = 8(rj_z/B_\theta)(q/rq') \sim 5$, typically. All islands with widths less than a certain critical width are stabilized. A feedback current density (expressed as a fraction of the unperturbed local current density j_{zo}) of $\tilde{j}_{rf}/j_{zo} \sim 0.05$-0.1 should be sufficient to suppress m = 2 islands with widths up to $w/a \sim 0.1$ in a typical case ($\Delta' a \sim 3$).

Stabilization of the m = 1 mode is more problematical, and it depends (theoretically) on the degree to which the m = 1 ideal-MHD internal kink can be made positively stable, for example, by triangularity of the cross section /4/. Detailed calculations /1/ indicate that the effective Δ' can be related (for a given current profile, in particular parabolic) to the triangular distortion ξ_{3a} of the plasma boundary: for $q(0) \sim 0.9$, we obtain

$$\Delta' a \sim 50/\xi_{3a}^2 .$$

Even for high values of triangularity ($\xi_{3a} \sim 0.5$), the effective $\Delta' a$-value will be about two orders-of-magnitude larger than typical values for the m = 2 mode. Values of C_d are, however, larger at the q = 1 surface, typically $C_d \sim 50$. Thus, feedback stabilization of the m = 1 mode by island current drive might lie just within the bounds of practicality ($\tilde{j}_{rf}/j_{zo} \sim 0.4$ for $w/a \sim 0.1$).

The remainder of this paper is devoted to a discussion of rf techniques for

achieving the required localization of the rf power.

III. FEEDBACK BY LOWER-HYBRID CURRENT DRIVE

We examine the feasibility of using lower-hybrid current drive to modify the current profile in magnetic islands in order to limit the size of the island by feedback. Since lower-hybrid current drive is known to work well, its feasibility as a feedback technique rests on practical details such as the spectrum control required for local deposition. This, in turn, is influenced by details of geometry and plasma profiles, which can be included in calculations based on geometric optics, i.e., the ray-tracing approach.

In this approach, a local dispersion relation, $D(\underline{r},\underline{k},\omega) = 0$, allows one to follow the position $\underline{r}$, wave vector $\underline{k}$, and power content P of a ray in time by integrating the following equations:

$$\dot{\underline{r}} = - \partial_{\underline{k}} D / \partial_{\omega} D,$$

$$\dot{\underline{k}} = + \partial_{\underline{r}} D / \partial_{\omega} D,$$

$$\dot{P}/P = - 2 \, \mathrm{Im} \, D / \partial_{\omega} D .$$

The physical content of the dispersion relation can vary according to the level of detail desired in the analysis. For example, for many purposes the lower-hybrid wave can be treated as electrostatic. In addition, current drive takes place only when lower-hybrid resonance is not a factor. In this case

$$D = (1 + \frac{\omega_{pe}^2}{\omega_{ce}^2})k_{\perp}^2 - \frac{\omega_{pe}^2}{\omega^2} k_{\parallel}^2 + i \frac{\omega_{pe}^2}{\omega^2} k_{\parallel}^2 \left[2\pi^{1/2} \left(\frac{\omega^2}{2k_{\parallel}^2 v_e^2}\right)^{3/2} \exp\left(-\frac{\omega^2}{2k_{\parallel}^2 v_e^2}\right)\right].$$

From this simplified form, one can see several important qualitative aspects of lower-hybrid propagation and damping. The phase velocity is primarily across the field ($k_{\perp} \gg k_{\parallel}$), and the group velocity is primarily along the field with a small component across the field:

$$(\dot{\underline{r}})_{\parallel} / (\dot{\underline{r}})_{\perp} = \frac{k_{\perp}}{k_{\parallel}} = \frac{\omega_{pe}/\omega}{(1 + \omega_{pe}^2/\omega_{ce}^2)^{1/2}} \approx \frac{\omega/k_{\parallel}}{\omega/k_{\perp}}$$

The imaginary term arises physically from Landau damping on electrons moving along the magnetic field. In this term, v_e is the electron thermal velocity, which is a function of position. The term is exponentially small at

the edge of the plasma where v_e is near zero, and damping reaches a maximum when $\omega^2/(2k_\parallel^2 v_e^2) = 3/2$.

To the extent that one can ignore gradients of plasma parameters along the field, $k_\parallel$ is constant over the path of the wave. Thus, in the simplest approximation, one selects a $k_\parallel$-value through the choice of physical dimensions of the wave coupler at the plasma edge, such that current driven from Landau damping is deposited at the desired location, either the q = 1 surface or the q = 2 surface. The correct phase, $\phi - q\theta$ (ϕ is the toroidal angle, θ is the poloidal angle), for depositing current is selected by launching the wave in proper synchronism with the rotation of the island. (If the island is not rotating, there is essentially no practical opportunity for interacting with the island in proper phase, because couplers are limited in number and fixed in position. In addition, detecting the island location is not possible with existing techniques if the island is stationary.)

The preceeding discussion indicates the basic plausibility of interacting with islands through lower-hybrid current drive. To go further, we need, first, to use the electromagnetic form of the dispersion relation for the lower-hybrid wave. This is because at some low $k_\parallel$, given roughly by $k_\parallel^2 c^2/\omega^2 \sim 1 + \omega_{pe}^2/\omega_{ce}^2$, there is a transformation to the fast wave, which has much different propagation and damping characteristics; low values of $k_\parallel$ will be of particular interest for interactions with the interior regions of hot plasmas. Second, we need to incorporate toroidal geometry, which causes $k_\parallel$ to evolve with the motion of the wave in response to variations in magnetic field strength along a ray trajectory.

These features are incorporated in a computer code that has been used for several years in analyzing lower-hybrid experiments on PLT. The dispersion relation used in the code contains electron Landau damping along the field, as already discussed, and ion Landau damping perpendicular to the field associated with very high perpendicular wave numbers near lower-hybrid resonance. The plasma model uses the toroidal coordinate system: r (minor radius), θ (poloidal angle), ϕ (toroidal angle). The equilibrium is approximated by flux surfaces of constant r, but there is no detailed pressure balance. Profiles of $n_{e,i}$ and $T_{e,i}$ are parabolas raised to a power. (The power is 1 for density, 1.4 for electron temperature, 2.0 for ion temperature.) The profile of q(r) is parameterized in terms of the central value q_o and the edge value q_a as follows:

$$q(r) = q_a(r^2/a^2)/[1 - (1 - r^2/a^2)^{q_a/q_o}.$$

Toroidal effects on $k_\parallel$ may be summarized as follows /5/. For very short paths from the launching point of a wave, $k_\parallel(R + r\cos\theta)$ is approximately constant, in accordance with approximate conservation of toroidal angular momentum. Thus, in the normal situation of a coupler on the outside mid-plane, $k_\parallel$ rises along the initial part of the ray trajectory. In contrast, for moderately long paths from the launching point of a wave, other toroidal effects produce the opposite, and usually dominant, behavior: $k_\parallel$ falls on moving to small major radius and rises on moving to large major radius. This effect is an important consideration for lower-hybrid feedback, since a rising $n_\parallel$ encourages local absorption by reducing the radial width of the Landau-resonance region. This favors placing the coupler on the top (bottom) of the torus rather than at the midplane.

For longer paths (possible only without strong damping), the wave always "bounces" off the cutoff region at low density with a random change in $k_\parallel$ at each bounce, but with a net up-shift in $k_\parallel$ for many bounces because $n_\parallel$ cannot go below unity. This effect has been used to account for the high efficiency of broadly distributed current drive. We do not wish to employ such effects here, since localization of the driven current would seem unlikely.

We choose parameters typical of PLT: $R = 1.35$ m, $a = 0.40$ m, $B = 3$ T, $q = 4.4$ ($I_p = 0.4$ MA), $\omega/2\pi = 2.45$ GHz, $n_e(0) = 5 \times 10^{13}$ cm^{-3}, $T_e(0) = 3.5$ keV, and deuterium ions with light impurities to make $Z_{eff} = 1.5$. We examine first the possibilities for interacting with the $m = 2$ mode, assuming $q = 1$ at the center of the plasma. In this case, the $q = 2$ surface is at ~25 cm minor radius, or 15 cm from the plasma edge. We find that $n_\parallel = 4$ produces the strongest damping near the $q = 2$ surface and that suitable localization of damping on the $q = 2$ surface remains for $\Delta n_\parallel \approx \pm 0.25$. To quantify the localization of damping relative to a given field line near the $q = 2$ surface, we plot in Fig. 3(b) the relative power remaining in the wave (P) versus total path length across field lines. (The path length across field lines is formed from the integral of $|\underline{dr} \times \underline{b}|$ along the ray, where $\underline{b}$ is a unit vector along the magnetic field.) In this manner, we find that the wave is absorbed within a distance of 4 cm measured across the field, after crossing the field for 12 cm. Figure 3(a) shows that the total path length along the field is approximately 250 cm, and the total damping distance is approximately 100 cm. The path is relatively short [see Fig. 3(d)] because the $q = 2$ surface is quite far out in the plasma. Accordingly, changes in the parallel wave number are modest, although visible [see Fig. 3(c)].

It is important to note that the large damping distance along the field apparent in Fig. 3(a) does not preclude adequate localization of the damping, because both ray path and magnetic island follow the field lines very closely. We also emphasize that Fig. 3(b) combines both radial and azimuthal contributions to the damping distance across the field.

Next, we consider interacting with a q = 1 surface. The model is the same except that we take q = 0.5 at the center of the plasma (a somewhat extreme case), leading to a q = 1 surface at about 17 cm where the temperature is 2.8 keV. In this case, the location of the wave launcher is quite important for effective localization of the driven currents.

The best results are obtained with launching from the bottom (or top). As shown in Fig. 4(b) a lower-hybrid wave with $n_{\parallel}$ = 2.5 deposits its power in 5 cm across field lines centered on the q = 1 surface. In doing so, the wave travels almost 500 cm along the field [Fig. 4(a)], while going 25 cm across the field [Fig. 4(d)]. The value of $n_{\parallel}$ rises to about 4 [Fig. 4(c)]. The band of $n_{\parallel}$-values for which damping is centered on the q = 1 surface has width $\Delta n_{\parallel} \sim$ 0.5, ranging from $n_{\parallel}$ = 2.25 to $n_{\parallel}$ = 2.75.

If the wave is launched from the outside mid-plane, the relatively long path length and toroidal effects on parallel wave number combine to prevent effective damping on the q = 1 surface on first encounter, no matter which value of $n_{\parallel}$ is chosen for the launched wave. Figure 5 shows the example of $n_{\parallel}$ = 2.5. Figure 5(a) shows the dispersion relation up to the point at which the calculation is stopped, at which point there has been very little absorption [Fig. 5(b)]. It is apparent from Fig. 5 that the wave becomes fast too soon to interact with the q = 1 surface, and it then enters a range of parameters where coupling to the fast mode is important. If the initial $n_{\parallel}$ is raised, damping occurs outside the q = 1 surface.

The analysis shows that ray tracing and linear theory allow the deposition of driven currents to be sufficiently narrow relative to a magnetic field line that the lower-hybrid wave can influence the island structure. Some effects *not included here which may bear on the practicality of this technique are:* broadening of the wave spectrum by edge turbulence; lengthening of the absorption distance by quasi-linear saturation of the wave-particle interaction; and the effect of the field structure of the island itself on the wave propagation. In addition, the successful interaction with the q = 1 island depends critically on the detailed prediction of ray tracing that $k_{\parallel}$ rises in a secular way for a wave moving to lower magnetic field. Experimental verification of this point has been slow to emerge from lower-hybrid

experiments. However, recent experiments on PLT /6/ show that comparisons of the current-drive efficiency of top and midplane couplers do match the predictions of the ray tracing code.

IV. FEEDBACK BY ELECTRON-CYCLOTRON HEATING

Electron-cyclotron heating can be used for feedback stabilization of magnetic islands in three distinct ways: localized heating; localized current drive; and provision of localized suprathermal electrons to enhance the local damping of LHCD. Electron-cyclotron heating that is localized just outside the $q = 2$ surface (but not feedback modulated) has been used successfully to suppress $m = 2$ modes /7/.

The accessibility of an ECH wave in a tokamak is well understood. From the low-field side, ECH power may be launched with the ordinary mode (O-mode) at fundamental resonance and with the extraordinary mode (X-mode) at any harmonic other than the fundamental. These outside-launched waves are best directed almost perpendicular to the toroidal magnetic field. For the fundamental O-mode the cutoff density is n_{cf} (n_{cf} is the density at which $\omega = \omega_{pe}$), and for the ℓth harmonic X-mode the cutoff density is $[(\ell-1)/\ell]n_{cf}$ for fixed frequency ω. From the high-field side, ECH power may be launched with the X-mode at fundamental resonance. For this case, the cutoff density is increased to a maximum of $2n_{cf}$, depending upon the injection angle with respect to the magnetic field.

The localization of ECH power deposition is fundamental for its application to feedback stabilization of magnetic islands. The degree of localization is related to the dimensionless "optical depth" τ, which is equal to $2\int_a^b k_i(s)ds$ (where s is the propagation arc length and k_i is the wave damping constant). The total single-pass absorption is given by $P_{abs} = P_{in}[1 - \exp(-\tau)]$. A detailed analysis for a Maxwellian plasma in a tokamak shows that τ is a function of R/λ_0, T_e/m_ec^2, n/n_{cf}, the resonant harmonic number ℓ, and the launch angle /8/.

When the optical depth τ is of order unity, the absorption width is determined by the larger of the Doppler broadening and the relativistic broadening of the resonance. For example, for the fundamental O-mode or the second harmonic X-mode in a PLT-size tokamak, the absorption width is roughly $10(T_e/m_ec^2)R$, and is determined by the relativistic broadening of the resonance. However, as τ becomes larger, the ECH power is absorbed before the resonance layer is reached, and there does not exist a simple formula for the

absorption width. However, a ray tracing code, in which a bundle of multiple rays at directions specified by the measured antenna pattern are followed, can be used to calculate the power deposition. When the optical depth τ becomes much larger than unity, the power will be almost totally absorbed on one side of the resonance, i.e., by electrons moving in a particular direction parallel to the magnetic field. As a result, direct current drive due to ECH absorption occurs.

Due to the relativistically shifted resonance condition, an X-mode wave launched from the high-field side will interact with the faster electrons first and, therefore, produce suprathermal electrons. By proper choice of the incident angle with respect to the magnetic field, the resonance condition produces a preferential interaction with particles moving in one parallel direction, creating a suprathermal electron population that is well suited for efficient coupling of LHCD.

In the following discussion, we apply these considerations to the case of PLT. With 60-GHz gyrotrons, the cutoff density for the fundamental O-mode is 4.4×10^{13} cm^{-3} and for the second harmonic X-mode is 2.2×10^{13} cm^{-3}. Thus, the near-poloidal-plane launch of the O-mode from the low-field side is suitable for suppression of the m = 1 mode in the denser central regions of the plasma. The same type of launch of the X-mode at the second harmonic is suitable for suppression of the m = 2 mode in the edge region of the plasma. Figure 6 shows ray tracing results for a fundamental O-mode launched from a realistic antenna on PLT. It is for an assumed parabolic density profile and "parabolic-squared" temperature profile, with a peak density of 4×10^{13} cm^{-3} and a peak temperature of 1.5 keV. Note that absorption occurs over a radial distance of ~5 cm. Since O-mode absorption is mainly collisional, i.e., involving thermal electrons, this technique is suitable mainly for feedback by island heating.

Top launch of the fundamental X-mode can also be used for access to the denser central region. When the temperature is high enough, the wave power can be deposited in a fairly localized region around a selected minor radius.

Since the optical depth is about four times larger for the second harmonic X-mode than for the fundamental O-mode at similar plasma parameters, the second harmonic X-mode at a low plasma density ($1\text{-}2 \times 10^{13}$ cm^{-3}) also has the possibility of providing localized ECH current drive.

The application of the second harmonic O-mode from the low-field side will result in very little absorption, and the transmitted power can be reflected and converted into the X-mode by a polarized reflector located at the inner

torus wall. With such an arrangement, it is possible to produce an effective X-mode launch from the high-field side at the second harmonic at a small angle (about 15°) with respect to the toroidal field. As a result, localized suprathermal electrons may be produced for enhanced efficiency and localization of LHCD. The top launch of the fundamental X-mode may also produce a similar effect for lower density plasmas.

We have modeled the effect of localized suprathermal electrons, for example from ECH, on lower-hybrid current drive. We find the effect can be made quite favorable. As an example, consider the case of Fig. 5, in which lower-hybrid power was unable to influence the q = 1 surface. If a suprathermal, electron population of 10^{10} cm^{-3} density and 12 keV peak temperature is added around the 15 cm radius location, then the current drive interaction is strong at the q = 1 surface. (See Fig. 7.)

V. CONCLUSIONS

Stabilization of low-m magnetic islands by rf current-drive feedback appears quite promising, and the feedback power required to suppress the m = 2 mode is modest. The feedback power needed to suppress the more rapidly growing m = 1 mode is much larger, and the ideal-MHD m = 1 mode must be positively stable -- implying a strongly shaped plasma cross section. The current-drive power must be modulated in phase with a mode-detecting signal. For optimum efficiency, the rf power must be locally deposited at the magnetic island, but the radial deposition width need not be as narrow as the island itself. Calculations based on ray tracing and linear absorption show that lower-hybrid current drive should be capable of providing adequately localized deposition at the q = 2 surface and (if a top launch is used) also at the q = 1 surface. Localized electron-cyclotron heating could be used for the (less efficient) technique of feedback by island heating or as an adjunct to lower-hybrid current drive. If restricted to an outside launch, electron-cyclotron current drive is difficult to achieve at high plasma densities. Near-term experiments on island feedback are possible, for example, in PLT.

ACKNOWLEDGEMENTS

The authors are grateful for useful discussions with H. P. Furth, A. H. Kritz, and R. B. White.

This work was supported by the United States Department of Energy Contract No. DE-AC02-76-CHO-3073.

REFERENCES

/1/ RUTHERFORD, P. H., in Course and Workshop on Basic Physical Processes of Toroidal Fusion Plasmas (Varenna, Italy, August 26-September 3, 1985), to be published.

/2/ FURTH, H. P., in Controlled Fusion and Plasma Physics (Proc. 12th Europ. Conf., Budapest, Hungary, September 2-6, 1985), to be published.

/3/ YOSHIOKA, Y., KINOSHITA, S., and KOBAYASHI, T., Nucl. Fusion 24 (1984) 565.

/4/ WHITE, R. B., in Workshop on Magnetic Reconnection and Turbulence (Cargese, France, July 7-13, 1985), to be published.

/5/ IGNAT, D. W., Phys. Fluids 24 (1981) 1110.

/6/ STEVENS, J. E., et al., Controlled Fusion and Plasma Physics (Proc. 12th Europ. Conf., Budapest, Hungary, September 2-6, 1985) to be published; also BERNABEI, S., et al., in Radio-Frequency Plasma Heating (Proc. 6th Topical Conf., Pine Mountain, Ga., May 13-15, 1985), to be published.

/7/ ALIKAEV, V.V., et al., in Plasma Physics and Controlled Nuclear Fusion Research (Proc. 10th Int. Conf., London, 1984), Vol. I, IAEA, Vienna (1985) 419.

/8/ BORNATICI, M., et al., Plasma Phys. 23 (1981) 1127.

FIGURE CAPTIONS

Fig. 1 Schematic illustration of q(r) and p(r) profiles for a "conventional" and "sawtooth-suppressed" tokamak. The sawtooth-suppressed tokamak could have q(0) as low as 0.7, and it would be expected to have a flat pressure profile within $q(r) < 1$.

Fig. 2 Schematic illustration of feedback stabilization of m = 1 rotating magnetic islands by rf heating or current drive using ECH or LHCD techniques.

Fig. 3 Interaction of lower-hybrid waves with the q = 2 surface.
(a) Relative power P remaining in the wave versus path length along the field. Damping distance measured along the field is ~ 100 cm.
(b) Relative power P remaining in the wave versus path length across the field (solid); 1/q versus path length across the field (dashed). Damping occurs in a distance of ~ 4 cm, centered on the q = 2 surface.
(c) $N_{\parallel}$ of wave versus radial position in the plasma. This shows a modest change in $N_{\parallel}$ due to toroidal effects. (d) Ray path in cross section of plasma.

Fig. 4 Interaction of lower-hybrid waves with the q = 1 surface using bottom launch to cause $N_{\parallel}$ to rise as the wave penetrates.
(a) Relative power P remaining in the wave versus path length along the field. Damping distance along the field is ~ 100 cm.
(b) Relative power P remaining in the wave versus path length across the field (solid); 1/q versus path across field (dashed). Damping occurs in a distance of ~ 4 cm centered on the q = 1 surface.
(c) $N_{\parallel}$ of wave versus radial position in the plasma. This shows a strong rise in $N_{\parallel}$ due to toroidal effects.
(d) Ray path in cross section of plasma.

Fig. 5 No interaction of lower-hybrid waves with q = 1 surface. Other launched values of $N_{\parallel}$ fail also: higher $N_{\parallel}$ is damped outside, while lower $N_{\parallel}$ is converted to the fast wave earlier.
(a) Dispersion characteristics at end point of ray where calculation was stopped after initial failure to damp.
(b) Relative power P remaining in the wave versus path length across the field (solid); 1/q versus path length across the field (dashed). Surfaces of q = 2 and q = 1 are crossed without damping.
(c) $N_{\parallel}$ of the wave versus radial position in the plasma. This shows significant changes in $N_{\parallel}$ due to toroidal effects. (d) Ray path in cross section of plasma.

Fig. 6 Power deposition in PLT with a 60 GHz, O-mode launch with a center ray at 6° from the perpendicular to the toroidal field direction. The antenna pattern is simulated by five rays at 3° intervals from the center ray (i.e., center ray, ± 3° in toroidal angle and ± 3° in poloidal angle). The ECH resonance is placed at 15 cm from the plasma center.

Fig. 7 Suprathermal electrons, supplied by ECH for example, cause strong interaction with the q = 1 surface with the same lower-hybrid wave which failed in Fig. 5.
(a) Temperature of suprathermal electrons versus radial position.
(b) Relative power P remaining in wave versus path length across the field (solid); and 1/q versus path length across the field (dashed).

#85A0092

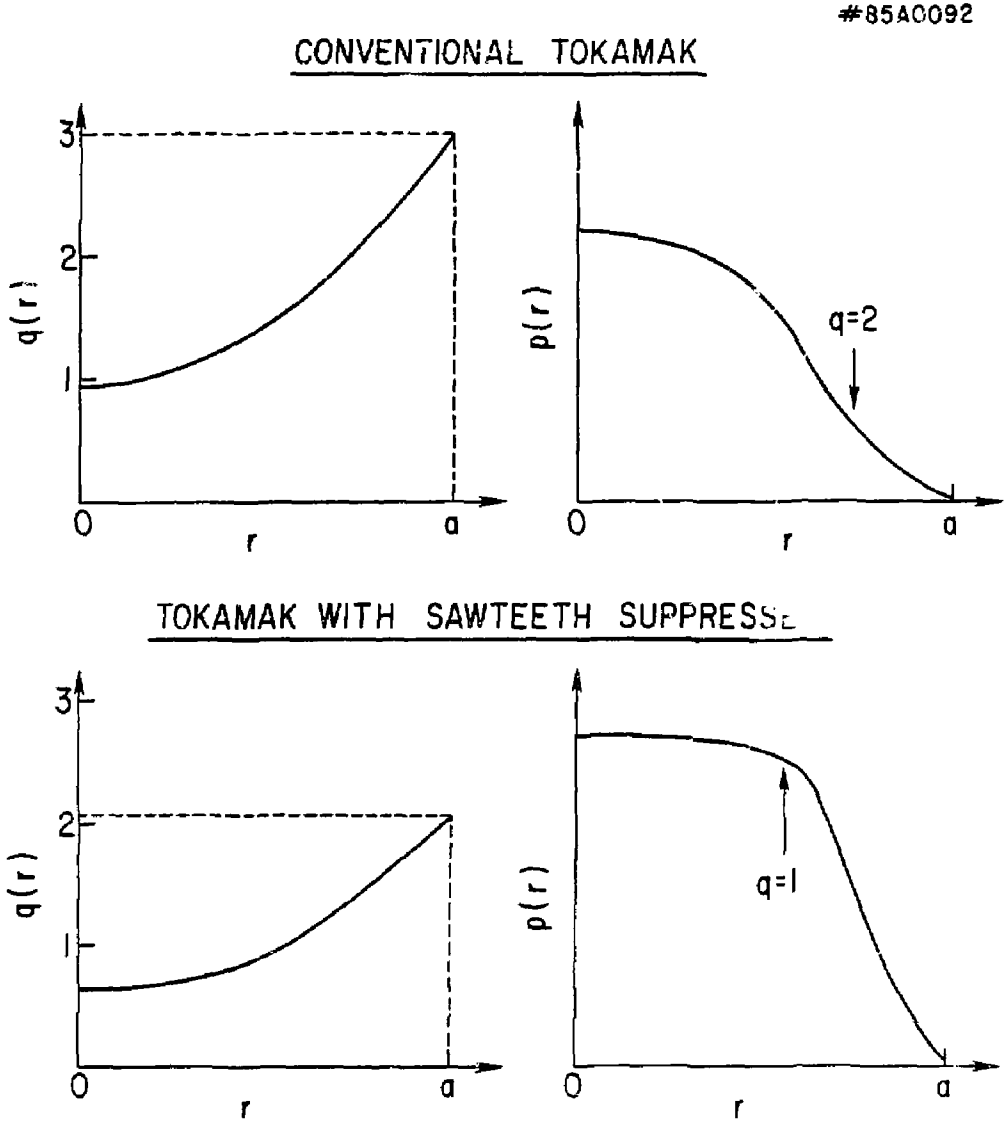

Fig. 1

#85A0050

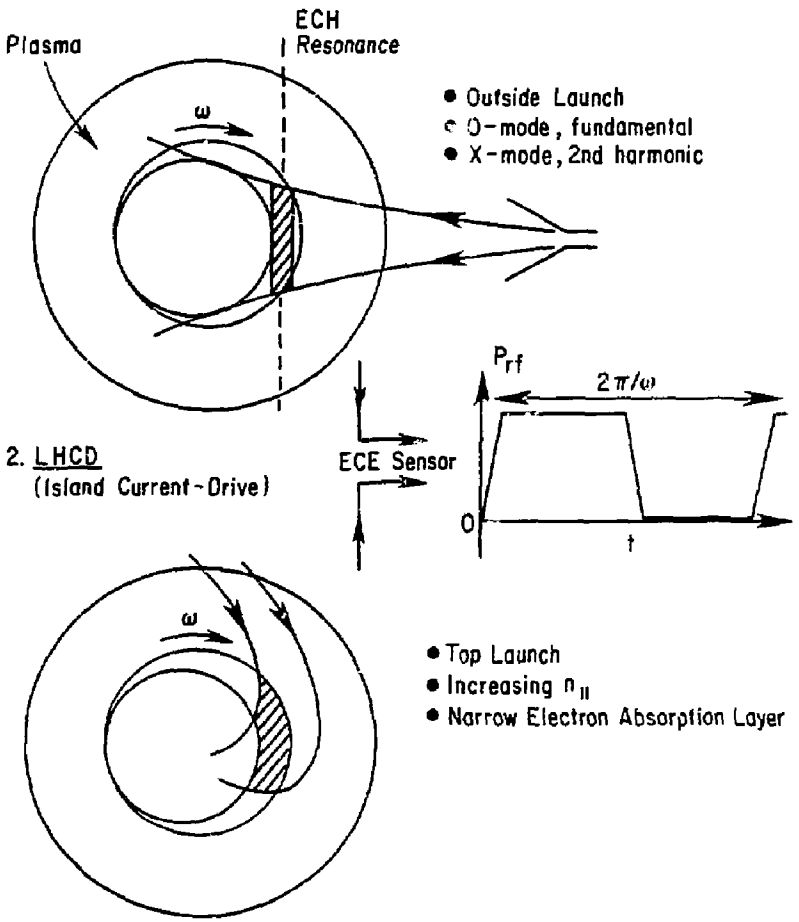

Fig. 2

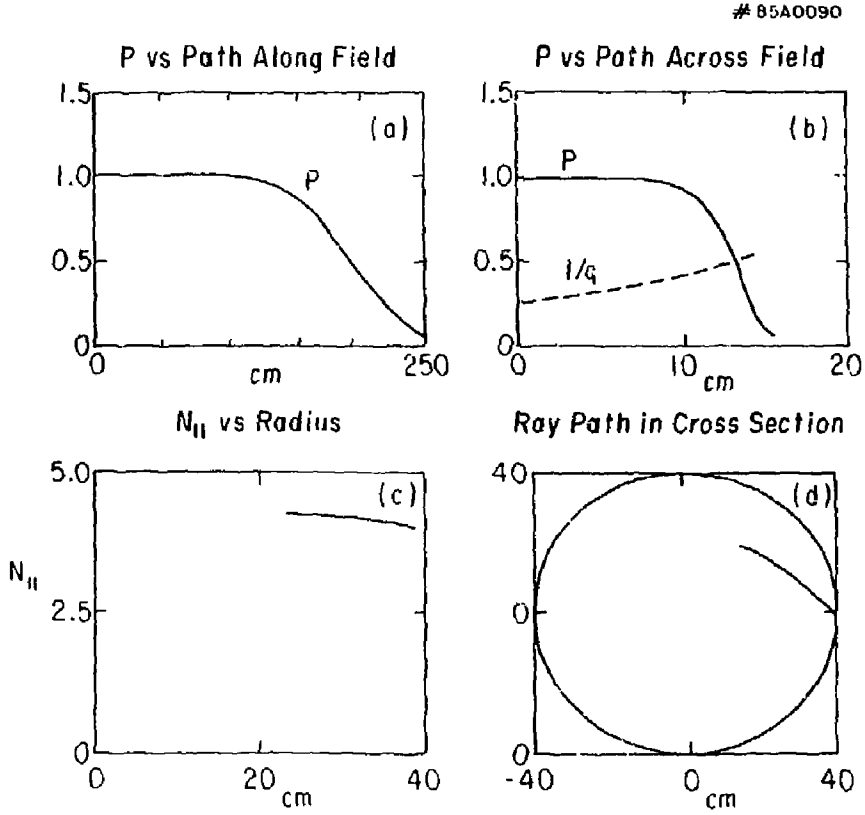
#85A0090
P vs Path Along Field
(a)
P
1.5
1.0
0.5
0
0
cm
250
P vs Path Across Field
(b)
P
1/q
1.5
1.0
0.5
0
0
10
cm
20
N|| vs Radius
(c)
N||
5.0
2.5
0
0
20
cm
40
Ray Path in Cross Section
(d)
40
0
0
-40
0
cm
40

Fig. 3

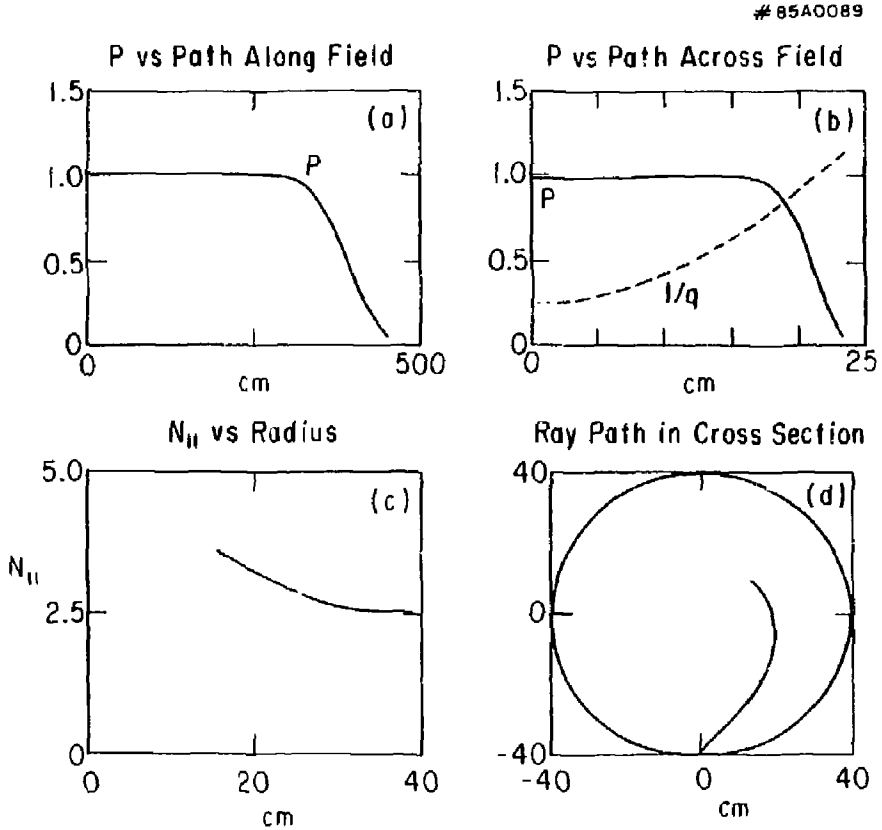
#85A0089
P vs Path Along Field
(a)
P
1.5
1.0
0.5
0
0
500
cm
P vs Path Across Field
(b)
P
1/q
1.5
1.0
0.5
0
0
25
cm
N∥ vs Radius
(c)
N∥
5.0
2.5
0
0
20
40
cm
Ray Path in Cross Section
(d)
40
0
-40
-40
0
40
cm

Fig. 4

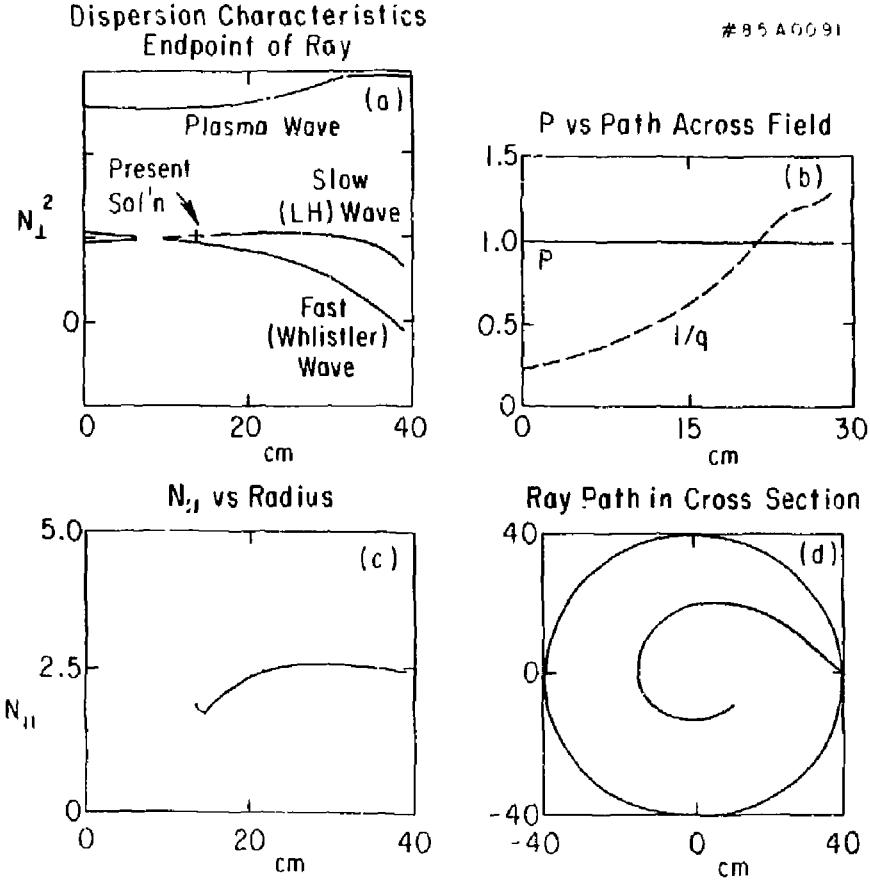
Dispersion Characteristics
Endpoint of Ray
#85A0091
(a)
Plasma Wave
Present
Sol'n
Slow
(LH) Wave
Fast
(Whistler)
Wave
$N_\perp^2$
0
20
40
cm
P vs Path Across Field
(b)
1.5
1.0
0.5
0
P
1/q
0
15
30
cm
$N_{/\!/}$ vs Radius
(c)
5.0
2.5
0
$N_{/\!/}$
0
20
40
cm
Ray Path in Cross Section
(d)
40
0
-40
-40
0
40
cm

Fig. 5

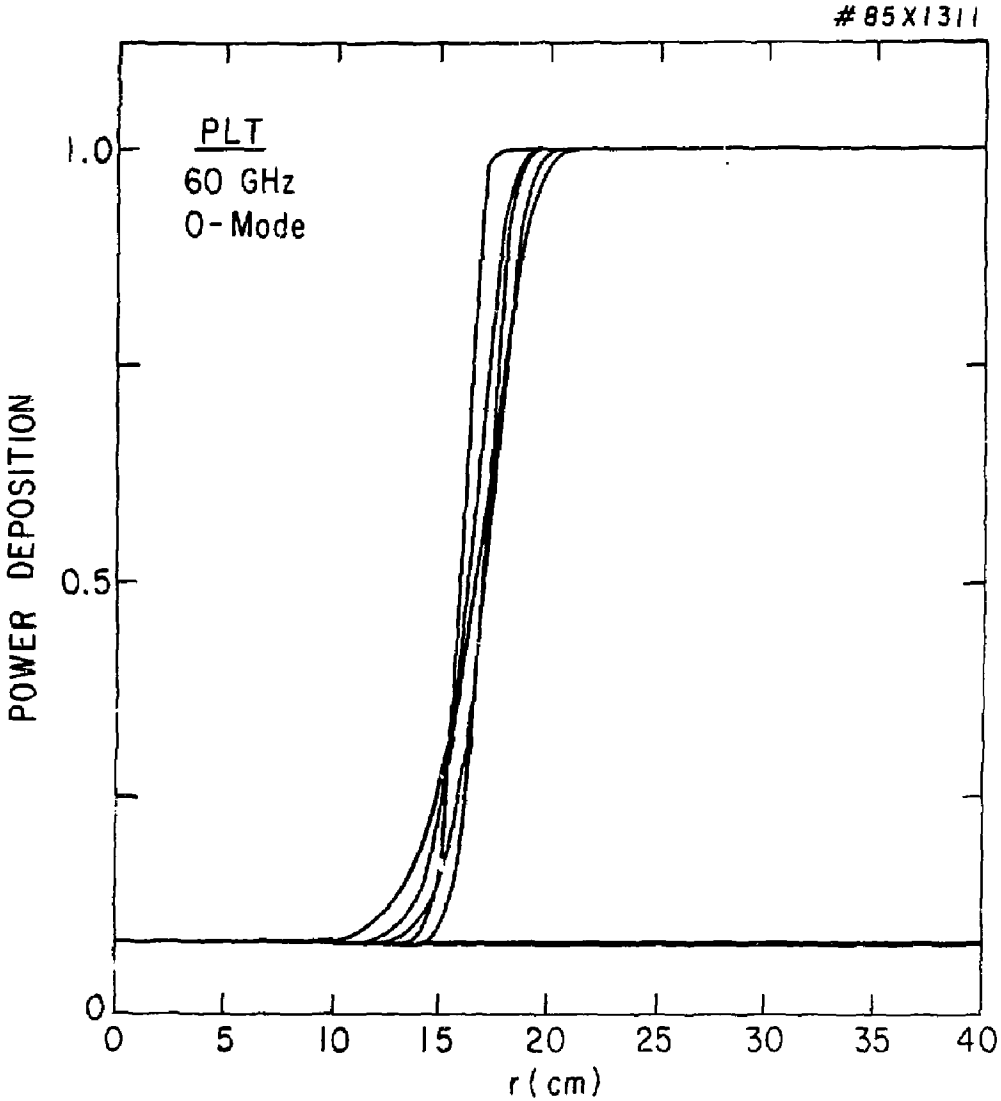
#85X1311
PLT
60 GHz
O-Mode
POWER DEPOSITION
1.0
0.5
0
0
5
10
15
20
25
30
35
40
r (cm)

Fig. 6

#85A0103

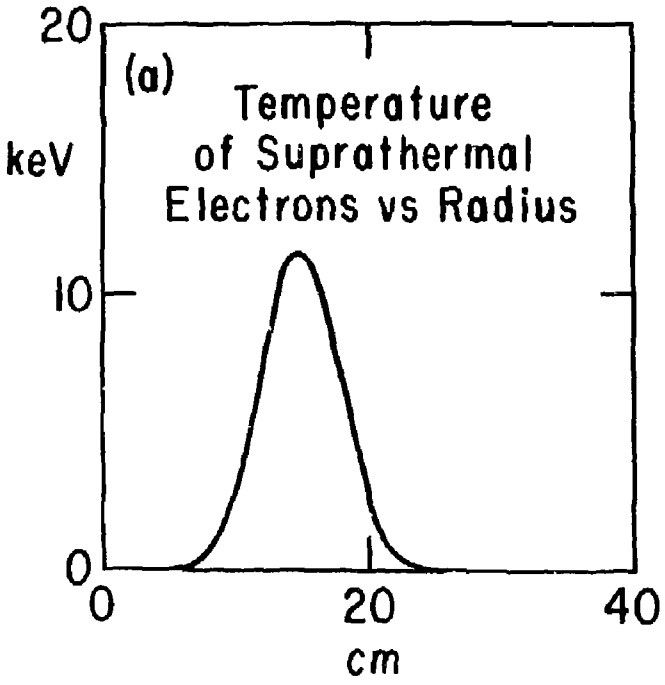

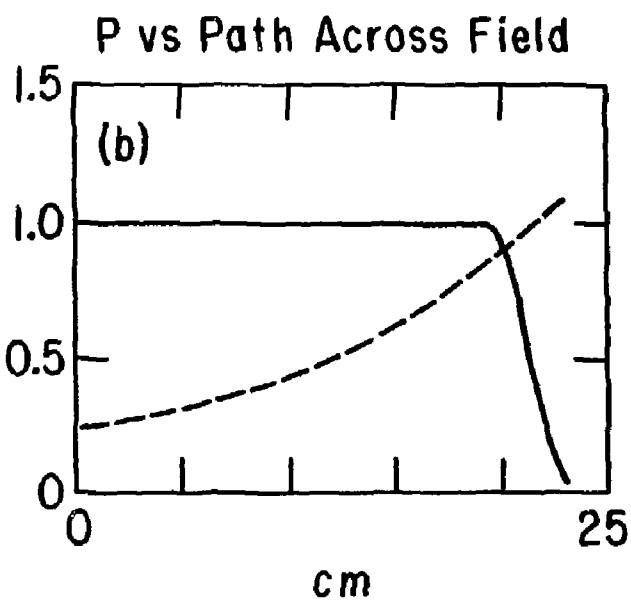

Fig. 7

EXTERNAL DISTRIBUTION IN ADDITION TO UC-20

Plasma Res Lab, Austra Nat'l Univ, AUSTRALIA
Dr. Frank J. Paoloni, Univ of Wollongong, AUSTRALIA
Prof. I.R. Jones, Flinders Univ., AUSTRALIA
Prof. M.H. Brennan, Univ Sydney, AUSTRALIA
Prof. F. Cap, Inst Theo Phys, AUSTRIA
Prof. Frank Verheest, Inst theoretische, BELGIUM
Dr. D. Palumbo, Dg XII Fusion Prog, BELGIUM
Ecole Royale Militaire, Lab de Phys Plasmas, BELGIUM
Dr. P.H. Sakanaka, Univ Estadual, BRAZIL
Dr. C.R. James, Univ of Alberta, CANADA
Prof. J. Teichmann, Univ of Montreal, CANADA
Dr. H.M. Skarsgard, Univ of Saskatchewan, CANADA
Prof. S.R. Sreenivasan, University of Calgary, CANADA
Prof. Tudor W. Johnston, INRS-Energie, CANADA
Dr. Hannes Barnard, Univ British Columbia, CANADA
Dr. M.P. Bachynski, MPB Technologies, Inc., CANADA
Chalk River, Nucl Lab, CANADA
Zhangwu Li, SW Inst Physics, CHINA
Library, Tsing Hua University, CHINA
Librarian, Institute of Physics, CHINA
Inst Plasma Phys, Academia Sinica, CHINA
Dr. Peter Lukac, Komenskeho Univ, CZECHOSLOVAKIA
The Librarian, Culham Laboratory, ENGLAND
Prof. Schatzman, Observatoire de Nice, FRANCE
J. Radet, CEN-BP6, FRANCE
AM Dupas Library, AM Dupas Library, FRANCE
Dr. Tom Mual, Academy Bibliographic, HONG KONG
Preprint Library, Cent Res Inst Phys, HUNGARY
Dr. R.K. Chhajlani, Vikram Univ. INDIA
Dr. B. Dasgupta, Saha Inst, INDIA
Dr. P. Kaw, Physical Research Lab, INDIA
Dr. Phillip Rosenau, Israel Inst Tech, ISRAEL
Prof. S. Cuperman, Tel Aviv University, ISRAEL
Prof. G. Rostagni, Univ Di Padova, ITALY
Librarian, Int'l Ctr Theo Phys, ITALY
Miss Clelia De Palo, Assoc EURATOM-ENEA, ITALY
Biblioteca, del CNR EURATOM, ITALY
Dr. H. Yamato, Toshiba Res & Dev, JAPAN
Direc. Dept. Lg. Tokamak Dev. JAERI, JAPAN
Prof. Nobuyuki Inoue, University of Tokyo, JAPAN
Research Info Center, Nagoya University, JAPAN
Prof. Kyoji Nishikawa, Univ of Hiroshima, JAPAN
Prof. Sigeru Mori, JAERI, JAPAN
Prof. S. Tanaka, Kyoto University, JAPAN
Library, Kyoto University, JAPAN
Prof. Ichiro Kawakami, Nihon Univ, JAPAN
Prof. Satoshi Itoh, Kyushu University, JAPAN
Dr. D.I. Choi, Adv. Inst Sci & Tech, KOREA
Tech Info Division, KAERI, KOREA
Bibliotheek, Fom-Inst Voor Plasma, NETHERLANDS
Prof. B.S. Liley, University of Waikato, NEW ZEALAND
Prof. J.A.C. Cabral, Inst Superior Tecn, PORTUGAL
Dr. Octavian Petrus, ALI CUZA University, ROMANIA
Prof. M.A. Hellberg, University of Natal, SO AFRICA
Dr. Johan de Villiers, Plasma Physics, Nucor, SO AFRICA
Fusion Div. Library, JEN, SPAIN
Prof. Hans Wilhelmson, Chalmers Univ Tech, SWEDEN
Dr. Lennart Stenflo, University of UMEA, SWEDEN
Library, Royal Inst Tech, SWEDEN
Centre de Recherchesen, Ecole Polytech Fed, SWITZERLAND
Dr. V.T. Tolok, Kharkov Phys Tech Ins, USSR
Dr. D.D. Ryutov, Siberian Acad Sci, USSR
Dr. G.A. Eliseev, Kurchatov Institute, USSR
Dr. V.A. Glukhikh, Inst Electro-Physical, USSR
Institute Gen. Physics, USSR
Prof. T.J.M. Boyd, Univ College N Wales, WALES
Dr. K. Schindler, Ruhr Universitat, W. GERMANY
Nuclear Res Estab, Julich Ltd, W. GERMANY
Librarian, Max-Planck Institut, W. GERMANY
Bibliothek, Inst Plasmaforschung, W. GERMANY
Prof. R.K. Janev, Inst Phys, YUGOSLAVIA